Clinical, Cosmetic and Investigational Dermatology

Dovepress
Taylor & Francis Group

Open Access Full Text Article

ORIGINAL RESEARCH

Effects of Exosomes From Hypoxia-Induced Adipose-Derived Stem Cells on Ameliorating Photoaging

Cuc Bach Huynh[1,2], Ngoc Bich Vu[1,3], Trung The Van[2], Phuc Van Pham[1,3]

[1]VNUHCM-US Stem Cell Institute, University of Science, Ho Chi Minh City, Vietnam; [2]Department of Dermatology, University of Medicine and Pharmacy at Ho Chi Minh City, Ho Chi Minh City, Vietnam; [3]Vietnam National University Ho Chi Minh City, Ho Chi Minh City, Vietnam

Correspondence: Trung The Van; Phuc Van Pham, Email trungvan@ump.edu.vn; phucpham@sci.edu.vn

Introduction: Photoaging, a significant concern in cosmetic dermatology, involves complex skin damage that necessitates effective treatments. Exosomes derived from adipose-derived stem cells (ADSCs), particularly those generated under hypoxic conditions (hypADSC-Exo), have emerged as a promising cell-free therapeutic approach. This study investigates the effects of hypADSC-Exo on reducing human dermal fibroblast (HDF) senescence and mitigating signs of photoaging through topical application in a mouse model.

Methods: Exosomes were isolated from hypoxia-induced human ADSCs via ultracentrifugation and identified using flow cytometry (CD9, CD63, CD81). Transmission electron microscopy (TEM) confirmed the vesicle morphology, while the Bradford assay and nanoparticle tracking analysis (NTA) assessed the protein content and size. In vitro, UV-induced senescent HDFs were treated with hypADSC-Exo. Cell morphology, senescence (SA-β-gal assay), proliferation (Alamar Blue), and gene expression (p16, p21 via qPCR) were evaluated. In vivo, photoaged mice received hypADSC-Exo treatments (50 or 100 μg/mL) twice weekly for six weeks. Skin parameters (wrinkles, thickness, hydration, elasticity) were evaluated biweekly. Skin biopsies were used to assess epidermal and dermal thickness, collagen density, and gene expression of collagen types 1, 3 and MMP-1, 2, and 3.

Results: hypADSC-Exo exhibited a cup-shaped morphology under TEM and expressed exosomal markers CD9, CD63, and CD81. In vitro, hypADSC-Exo improved HDF morphology, reduced SA-β-gal activity, enhanced proliferation, and downregulated p16 and p21. In vivo, it reduced skin wrinkles and thickness. Treated mice exhibited improvement in hydration, elasticity, decreased epidermal and dermal thickness, and increased collagen density. Collagen types 1 and 3 increased slightly, while the levels of MMP-1, 2, and 3 decreased in the exosome group.

Conclusion: Our findings demonstrate that hypADSC-Exo reduces senescence in UV-induced aged HDF and improves photoaging in mice. These effects likely result from decreased MMP-1, 2, 3 expression and increased collagen deposition, making hypADSC-Exo a promising therapy for photoaging.

Keywords: hypoxic exosome, adipose-derived stem cell, senescent dermal fibroblast, photoaging

Introduction

Skin aging is a complex process influenced by both intrinsic and extrinsic factors, resulting in irreversible degradation of skin structure and function. Intrinsic aging arises from physiological cellular changes and the accumulation of metabolic byproducts over a lifetime,[1] while extrinsic aging encompasses harmful effects from environmental components, such as ultraviolet (UV) radiation, smoking,[2,3] air pollution,[4] and nutritional imbalances.[2,5,6] Among these, UV radiation from sunlight is a significant contributor to photoaging.[7] Both UVA (315–400 nm) and UVB (290–315 nm) rays are responsible for specific characteristics of photoaging, including skin roughness, dryness, deep wrinkles, pigmentation disorders, and laxity.[8]

Research has identified the accumulation of senescent human dermal fibroblasts (HDF) as a key feature of skin aging.[9] These senescent fibroblasts are prevalent in photoaged skin, resulting in reduced collagen production and increased secretion

Received: 20 February 2025
Accepted: 2 July 2025
Published: 9 July 2025

of inflammatory cytokines and matrix metalloproteinases (MMPs). Elastosis, marked by degraded elastin fibers in the superficial dermis, is a hallmark of photoaging, detectable through clinical observation and histological evaluation.[10]

Currently, small extracellular vesicle or exosome therapy shows great promise as a novel approach for effectively treating and preventing photoaging. Exosomes are lipid bilayer nano-sized vesicles secreted by various cells, ranging in size from 30 nm to 150 nm. They appear as cup-shaped structures under negative staining in conventional transmission electron microscopy (TEM), while cryo-TEM reveals their spherical shape in solution.[11] These vesicles contain multiple bioactive components, including lipids, proteins, and nucleic acids, facilitating cell-cell communication. Exosomes can be easily internalized by target cells, delivering their cargo effectively. Their functions include regulating cellular interactions and contributing to processes such as cancer invasion, the coagulation system, immune regulation, and angiogenesis, as well as serving as vehicles for drug or gene delivery.

Numerous studies have highlighted the therapeutic potential of exosomes derived from stem cells in treating dermatological conditions, including tissue regeneration, wound healing, inflammatory diseases, and aging disorders.[12] The therapeutic effects of these exosomes are largely due to their immunomodulatory and anti-inflammatory properties, which improve cell senescence, induce angiogenesis,[13,14] reduce oxidative stress, and enhance the synthesis of extracellular matrix (ECM) components.[15,16] Exosomes from human adipose-derived stem cells (ADSC-Exo) improve senescent HDF by reducing senescence-associated β-galactosidase (SA-β-Gal) activity, inhibiting senescence-related proteins like p53, p21, and p16, and promoting HDF migration. They also increase type I collagen expression and downregulate reactive oxygen species (ROS).[17] Cell cycle analysis has shown that ADSC-Exo enhances the proportion of cells in the S-phase. Key microRNAs in ADSC-Exo, including hsa-miR-4484, hsa-miR-619-5p, and hsa-miR-6879-5p,[18] play vital roles in HDF regeneration. Furthermore, ADSC-Exo prevents photoaging by suppressing UVB-induced DNA damage and reducing ROS and MMP-1 through Nrf2 and MAPK/AP-1 pathway regulation. It may also activate the TGF-β/Smad pathway to increase type I procollagen levels.[19] Studies have indicated that miR-1246 in ADSC-Exo inhibits the MAPK/AP-1 signaling pathway to reduce MMP-1 production while activating the TGF-β/Smad pathway, promoting procollagen type 1 secretion and exerting anti-inflammatory effects.[20] These findings suggest that ADSC-Exo, through the paracrine activity of stem cells, can mitigate photoaging.

Recent research has shown that hypoxic conditions ($O2 < 5\%$)[21] can significantly enhance the survival and proliferation of stem cells compared to normoxic conditions.[22] Hypoxia can regulate factors in cellular adaptation, including non-coding RNA, messenger RNA (mRNA), proteins, and lipids in hypoxic cells exosomes.[23] Circ-Snhg11 in hypoxic ADSC exosomes inhibit hyperglycemia-induced endothelial cell damage and promotes M2-like macrophage polarization via miR-144-3p/HIF-1α axis.[24] Hypoxia also alters the size, quantity, quality, and therapeutic effects of exosomes produced by these stem cells.[21,25] Studies indicate that hypoxia-induced ADSCs produce larger vesicles[26] and secrete more exosomes. Hypoxic ADSC-Exo enhances angiogenesis through factors such as vascular endothelial growth factor (VEGF) and hypoxia-inducible factor (HIF-1α), while also reducing inflammation.[22] Additionally, hypoxic ADSC-Exo promotes proliferation, collagen metabolism, and migration in HDFs through the PI3K/AKT signaling pathway.[27] It has also been shown to mitigate UVB-induced vascular injury by reversing reactive oxygen species, inflammatory factor expression, and excessive collagen degradation via GLRX5 upregulation.[28]

However, the effects of hypoxic ADSC-Exo on mitigating skin photoaging have not yet been thoroughly investigated. This study aims to explore the therapeutic effects of human hypoxic ADSC-Exo on senescent HDF in vitro and photoaging in vivo using mouse models. The objectives are to isolate hypoxic ADSC-Exo with potent anti-photoaging capabilities and to rejuvenate photoaged skin in mice. This research hopes to illuminate the potential of hypoxic ADSC-Exo as a functional agent against photoaging.

Materials and Methods

Hypoxic Exosome Isolation

Human adipose-derived stem cells (hADSCs) were sourced from the Stem Cell Institute's Cell Bank, University of Science, VNU-HCM, Vietnam. The hADSCs at passage five were cultured in MSCCult II medium (Regenmedlab, Ho Chi Minh City, Vietnam), which consisted of DMEM/F12 supplemented with epidermal growth factor (EGF), fibroblast growth factor (FGF), and platelet-derived growth factor (PDGF), under hypoxic conditions (1% O2, 5% CO2) for

24 hours to collect the culture media for the isolation of exosome. hypADSC-derived exosomes (hypADSC-Exo) were isolated using ultracentrifugation (Beckman Coulter, USA). In brief, the supernatant (100 mL) was centrifuged at 300 × g for 10 minutes, followed by 2000 × g for another 10 minutes at 4 °C to remove dead cells and debris. Subsequently, the supernatant was centrifuged at 10,000 × g for 30 minutes and at 100,000 × g for 70 minutes to collect the exosome pellets at 4 °C. The pellets were then washed with 30 mL phosphate-buffered saline (PBS) by centrifuging at 100,000 × g for 70 minutes. The final pellets were collected and resuspended in PBS and used for subsequent experiments within 24 hours.

Hypoxic Exosome Identification

Exosome pellets obtained from 100 mL of supernatant were re-suspended in 100 µL filtered PBS for each characterization experiment. The morphology of hypADSC-Exo was evaluated using transmission electron microscopy (TEM). The size distribution and concentration of the exosomes were measured via nanoparticle tracking analysis (NTA) using the Nanotrac Flex system (Microtrac MRB, USA). The protein concentration of the exosomes was determined using the Bradford protein assay (Sigma, USA) according to the manufacturer's protocol. Exosomal marker proteins, including CD9, CD63, and CD81, were analyzed through flow cytometry (BD FACSMelody™ Cell Sorter, BD Biosciences, USA) using vesicles pre-attached to Aldehyde/Sulfate Latex Bead (Thermo Fisher Scientific, USA) and labeled with different fluorescence-labeled antibodies: anti-CD9-PE, anti-CD63-PE, and anti-CD81-APC (eBioscience, USA).

Fibroblast Isolation and Characterization

Human dermal fibroblasts (HDFs) were isolated from redundant abdominal skin samples obtained from abdominoplasty cosmetic surgery, with written informed consent from the patients and approval from the Ethics Committee at the University of Medicine and Pharmacy Ho Chi Minh City (approval no. 56/HĐĐĐ-ĐHYD, dated 28/01/2021). The isolation and characterization procedures followed previous methodologies.[29] Briefly, skin tissue was cut into small fragments, removed epidermis layers, and placed in a culture flask. HDFs were cultured from the skin samples in HFCult Medium (Stem Cell Institute, Viet Nam). The medium was refreshed every three days. After reaching 70–80% confluency, HDFs were collected using 0.05% trypsin-EDTA (Gibco) and prepared for subsequent experiments. Cells were characterized using fibroblast markers such as CD90, Vimentin, and S100A4, analyzed by flow cytometry (BD FACSCalibur™, BD Biosciences, USA). Fibroblasts at the fourth passage were selected for experiments.

UV Exposure to Fibroblasts

To induce senescence in HDFs, a Reptile UVB 100 compact 25W lamp (Exo Terra, USA) was used. The lamp was consistently positioned 10 cm above the culture plate surface. Prior to exposure, the UV lamp was warmed up for 10 minutes to ensure stable conditions, and UV doses were measured using two UV-AB meters: the Extech UV-AB light meter (model UV505; Wilsonville, USA) and the Santacary XAR-UV UVB light meter (Guangdong, China). The total irradiation dose consisted of UVB 1170 mJ/cm² plus UVA 720 mJ/cm² for 15 minutes, which is the sublethal dose established in the previous study.[29] The culture medium was removed, and cells were washed twice with PBS before UV-AB irradiation, which was conducted under a thin layer of PBS 1X to prevent drying. Following UV exposure, cells were rinsed again with PBS and incubated immediately in fresh culture media with serum for 72 hours. At this point, senescent cells were cryopreserved using a cryopreservation medium (Cryosave I, Stem Cell Institute, Vietnam) and prepared for further experiments. In the previous study, cellular senescence was also assessed based on several criteria, including changes in cell morphology and size, senescence-associated β-galactosidase (SA-β-gal) activity, reduced metabolic activity, and alterations in the gene expression of collagen I, collagen III, MMP3, p16, and p21.

Senescent Fibroblast Morphology After Treatment

Senescent HDFs (5×10^3 cells) were treated with 100 µL of hypADSC-Exo (10 µg/mL) or PBS and incubated in media for 24, 48, and 72 hours to assess the anti-senescent effects. Cell morphology was evaluated using inverted microscopy and captured using AxioVision 4.8 software. To measure cell size, HDFs were detached from the culture plate surface using Trypsin-EDTA 0.25% (Sigma -Aldrich, USA), then centrifuged at 300 × g to remove the supernatant and

resuspended in fresh culture medium. Images of suspended fibroblasts were captured under inverted microscopy, and cell sizes were measured using AxioVision 4.8 software. This experiment had two biological replications with a total of 16 cells to be counted per group at each time.

Senescence-Associated β-Galactosidase (SA-β-Gal) Staining

SA-β-Gal staining was employed to evaluate the effects of hypADSC-Exo on the senescence of HDFs. To accomplish this, HDFs were seeded at a density of 1×10^4 cells per well in 48-well plates and incubated at 37°C with 5% CO2. Cells in the hypADSC-Exo group received 100 μL of hypADSC-Exo (10 μg/mL), while the PBS group was given an equal volume of filtered PBS for 72 hours. Following this, the cells were fixed using 0.125 mL of Fixative Solution (ab102534, Abcam, UK) at room temperature for 15 minutes, then stained using the Staining Solution Mix from the SA-β-Gal staining kit (ab102534, Abcam, UK) as per the manufacturer's instructions. Positive senescent cells, which were stained blue, were observed under an inverted microscope. Two wells per group were captured, and the quantification of SA-β-Gal staining was analyzed using ImageJ (National Institutes of Health, USA).

Cell Proliferation Assay Post-Treatment

UV-induced senescent HDFs were divided into two groups: one treated with hypADSC-Exo and the other with PBS. Each group consisted of three technical replicates, seeded at a density of 5×10^3 cells per well in 96-well plates, and cultured in 100 μL of HFcult Medium. Cells in the hypADSC-Exo group received 100 μL of hypADSC-Exo (10 μg/mL), while the PBS group received an equal volume of filtered PBS for 72 hours. Cell proliferation was assessed using the Alamar Blue assay (Resazurin sodium salt, Sigma-Aldrich, USA) according to the manufacturer's guidelines. At 0, 24, 48, and 72 hours, 10 μL of Alamar Blue solution was added to each well, and the cells were incubated at 37°C for one hour. The absorbance was then measured at 595 nm using a microplate reader (DTX 880 multimode detector, Beckman Coulter, USA).

Animals and Ethical Approval

This study utilized female BALB/c mice aged six to eight weeks, sourced from the Laboratory for Animal Care and Use (LACU) at the Stem Cell Institute, University of Science, VNU-HCM, Vietnam. The mice were acclimatized for one week under controlled conditions (22°C ± 2°C, 55% humidity) with a 12-hour light/dark cycle. All experimental procedures adhered to LACU guidelines and ethical approval were granted by the Institutional Animal Care and Use Committee of the Stem Cell Institute (approval no. 210103/SCI-AEC, dated 20/01/2021).

Establishment of Photoaging Animal Model

Sixty female BALB/c mice were selected to create a photoaging model by the following protocol. Briefly, a UV lamp (UVB150, 18W-60cm, PT2396, Exo Terra, Canada) emitting both UVA and UVB light (290–370 nm) was positioned 30 cm from the backs of the animals. The lamp's energy output was calibrated using an Extech UV-AB light meter (model UV505, Wilsonville, USA) and a Santacary XAR-UV UVB light meter (Guangdong, China). Irradiation doses were set at 1080 mJ/cm² UVA and 115.2 mJ/cm² UVB, administered for sixty minutes daily, four consecutive days each week for 12 weeks. The total accumulated doses reached 51.8 J/cm² UVA and 5.53 J/cm² UVB. Before irradiation, the dorsal skin of the mice was shaved over an area of 8 cm² (2.0 x 4.0 cm), with shaving repeated every two weeks. Following exposure, the mice were prepared for treatment experiments.

Treatment in Mice

The mice were randomly assigned to six groups (n=10 per group) as follows: (1) normal group with no UV exposure (Normal group), (2) UV exposure without treatment (UV group), (3) UV exposure followed by topical application of 100 μL PBS (PBS group), (4) UV exposure followed by topical application of 100 μL hypADSC-Exo at 50 μg/mL (Exo1 group), (5) UV exposure followed by topical application of 100 μL hypADSC-Exo at 100 μg/mL (Exo2 group), and (6) UV exposure followed by topical application of 5 mg tretinoin cream at 0.05% (Tretinoin group). The 100 μL of PBS or hypADSC-Exo was applied to an 8 cm² area of the dorsal skin of each mouse with a 2-minute massage, after which the

area was covered with a transparent film dressing (Tegaderm, 3M, USA) for 1 hour to prevent licking and enhance epidermal penetration. This treatment was repeated every other day (Tuesdays and Fridays) for six weeks. For the tretinoin group, 5 mg of 0.05% tretinoin cream (Retacnyl, Galderma, Switzerland) was applied similarly. An additional group of eighteen to twenty-week-old normal mice served as the normal control, which subjected all the same handling. One week after the final administration of exosomes, the mice were sacrificed, and skin tissues were collected for further analysis.

Evaluation of Skin Appearance and Barrier Functions

Wrinkle Formation

The effectiveness of exosome treatment on skin aging was assessed by evaluating wrinkle formation. This assessment was performed by two independent observers every two weeks until week 6. The treated dorsal area was photographed while the mice were in a static position, using a pocket microscope (magnification, x100). Wrinkle formation was evaluated based on the scoring system established by Bissett et al[30] which includes four levels: Grade 0 (no coarse wrinkles), Grade 1 (few shallow coarse wrinkles), Grade 2 (some coarse wrinkles), and Grade 3 (several deep coarse wrinkles).

Skin Hydration Measurement

Mice were acclimatized in a controlled environment at 22°C and 55% humidity for 30 minutes before measurement. Skin moisture content was assessed using a Corneometer® CM825 probe (Courage + Khazaka electronic GmbH, Köln, Germany), which was placed in contact with the dorsal skin surface and slightly pressed to record the moisture level, in accordance with the manufacturer's instructions. Three technical replications were performed for each mouse at each time point.

Pinch Test for Skin Elasticity

The dorsal skin of each mouse was gently pinched with the thumb and index fingers to the highest point possible without lifting the mouse. The time (in seconds) for the skin to return to its normal state after release was recorded. Three technical replications were performed for each mouse at each time point.

Skinfold Thickness Measurement

Skinfold thickness was measured using a digital caliper (Mitutoyo, Japan). The back skin of the shaved mice was pinched manually, and the caliper was applied to the pinch, with three replicate measurements taken from three random areas on the shaved skin.

Histological Analysis

Histological analysis was conducted to evaluate epidermal thickness, dermal thickness, and collagen content. Dorsal skin tissues (1.0 x 1.0 cm) from each experimental group were collected and fixed in 10% formalin (Xilong, China) for 48 hours. Hematoxylin & eosin (H&E) staining (Thermo Scientific, USA) was utilized to assess epidermal and dermal thickness, while Masson's trichrome staining (Abcam, USA) was employed for collagen content analysis. Photographs of each stained sample slide were captured at three randomly selected regions using a camera attached to a digital optical microscope. Epidermal thickness was measured from the top of the stratum corneum to the bottom of the basal keratinocyte layer in five randomly selected fields from each photograph. Dermal thickness was assessed by measuring the distance from the bottom of the basement membrane to the top of the hypodermis. All stained sample images were analyzed using AxioVision Rel. software version 4.8 (Carl Zeiss, Thailand) for thickness calculations. Collagen fibers in Masson's trichrome-stained images were analyzed using ImageJ software (National Institutes of Health, USA) with the color deconvolution plugin for quantifying collagen content.[31]

Gene Expression Analysis

Skin samples (1.0 x 1.0 cm, which the depth was taken from the epidermis to the end of the dermis), were collected and preserved at −86°C for subsequent analysis. Total RNA was extracted from mouse skin tissue or cells (1 × 10^6 cells)

Table 1 Mouse Primer Sequences for Real-Time Quantitative Polymerase Chain Reaction

Target Gene	Sequences (5′–3′)	Sequence Length (mer)	Reference
COL1A1	F: CCGAACCCCAAGGAAAAGA R: CTGTTGCCTTCGCCTCTGA	19	NM_007742.4
COL3A1	F: TGGTCCTCAGGGTGTAAAGG R: GTCCAGCATCACCTTTTGGT	20	NM_009930.2
MMP1	F: AAGGCGATATTGTGCTCTCC R: CCTCATTGTTGTCGGTCCAC	20	NM_032007.3
MMP2	F: CAGGGAATGAGTACTGGGTCTATT R: ACTCCAGTTAAAGGCAGCATCTAC	24	NM_008610.3
MMP3	F: CATCCCCTGATGTCCTCGTG R: CTTCTTCACGGTTGCAGGGA	20	NM_010809.3
GAPDH	F: CCCACTAACATCAAATGGGG R: ACACATTGGGGGTAGGAACA	20	NM_001411840.1

Abbreviations: F, forward; R, reverse; COL1A1, collagen type I alpha 1 chain; COL3A1, collagen type III alpha 1 chain; MMP, matrix metalloproteinase; GAPDH, Glyceraldehyde-3-Phosphate Dehydrogenase.

Table 2 Human Primer Sequences for Real-Time Quantitative Polymerase Chain Reaction

Target gene	Sequences (5′–3′)	Sequence Length (mer)	Reference
hGAPDH	F: AATGGGCAGCCGTTAGGAAA R: GCGCCCAATACGACCAAATC	20	NM_001256799.3
P16	F: CATAGATGCCGCGGAAGGT R: CTAAGTTTCCCGAGGTTTCTCAGA	19	AH005371.3
P21	F: CTTCGACCTTTGTCACCGAGA R: AGGTCCACATGGTCTTCCTC	21	BC000312.2

Abbreviations: F, forward; R, reverse; GAPDH, Glyceraldehyde-3-Phosphate Dehydrogenase.

using the phenol-chloroform method with the easy-BLUE Total RNA Extraction Kit (Boca Scientific Inc., Dedham, MA, USA). Real-time quantitative RT-PCR was performed using the Luna Universal qPCR Master Mix (New England Biolabs, Ipswich, MA, USA) with primer sequences listed in Tables 1 and 2, following the manufacturer's protocol. Results were reported as relative quantity values of the target genes, calculated using the 2^(−ΔΔCt) method,[32] with normalization to GAPDH.

Statistical Analysis

Statistical analysis was conducted using GraphPad Prism version 10 (GraphPad, USA). Data are presented as mean ± standard deviation (SD) or mean ± standard error (SE) from at least two independent experiments. Comparisons between the two groups were performed using the Mann–Whitney test. For comparisons involving more than two groups, two-way ANOVA with Tukey's multiple comparison post-hoc test was employed. Differences were considered statistically significant at $p < 0.05$.

Results

Characterization of hypADSC-Exo

Transmission electron microscopy revealed that exosomes exhibited a cup-shaped morphology and nanosized vesicle structure (Figure 1A and B). The Bradford staining method indicated that the exosomal proteins isolated from 100 mL of

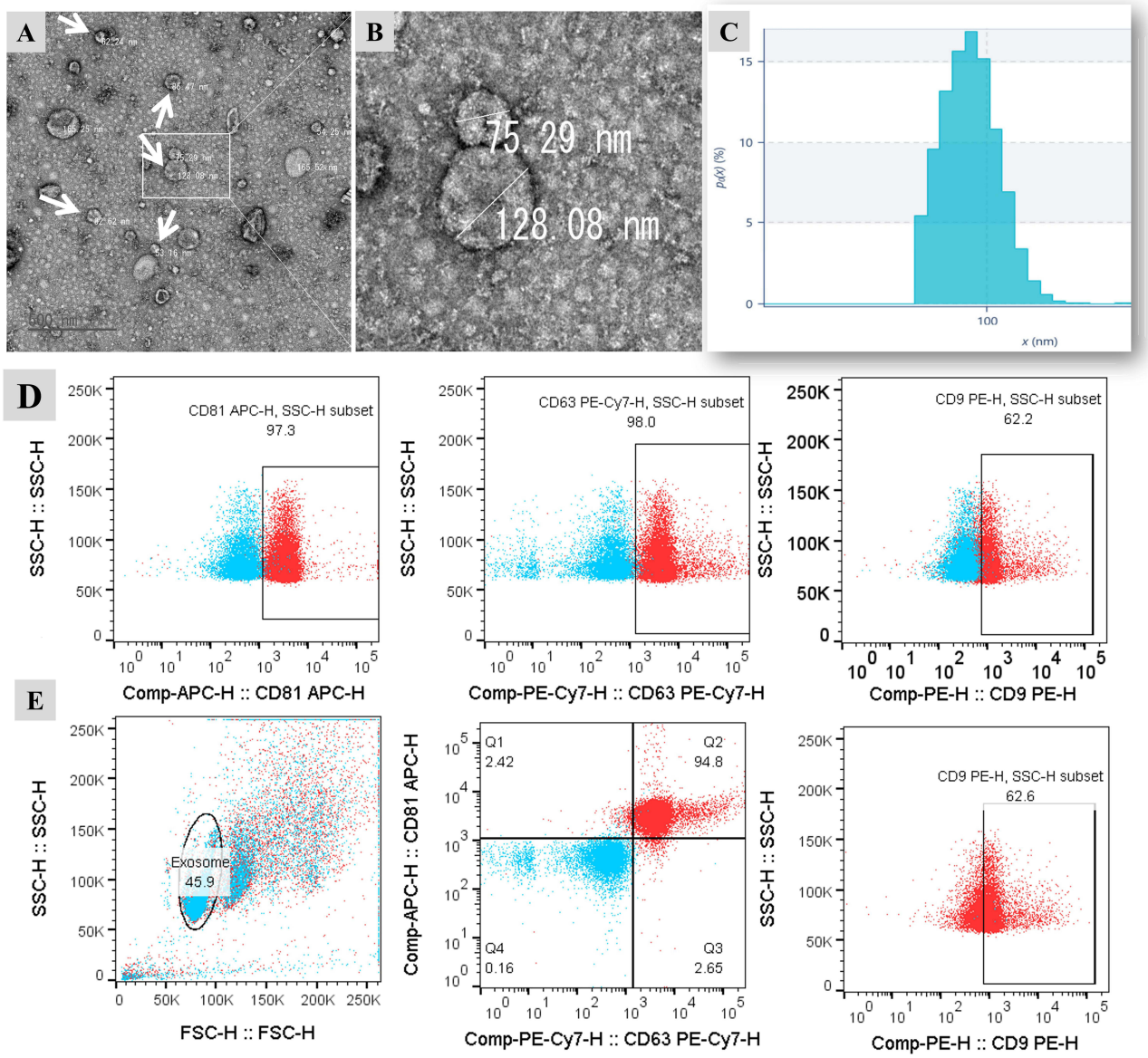

Figure 1 Characterization of hypADSC-Exo. The morphology and size of hypADSC-Exo under the TEM (**A** and **B**). Nanoparticle tracking analysis (NTA) assessed the size and density of the exosomes (**C**). Flow cytometry analysis for CD9, CD63, and CD81 exosomal markers (**D** and **E**). Characterization of hypADSC-Exo data represents a single technical replicate from two independent samples.

ADSC-derived conditional media amounted to approximately 80.4 μg. Nanoparticle tracking analysis (NTA) measured the mean size of hypADSC-Exo to be 102.3 ± 35.4 nm, with an exosome concentration of 7.024×10^{10} particles/mL (approximate 8.7×10^{8} particles/μg protein) (Figure 1C). Flow cytometry analysis confirmed that these vesicles expressed exosomal surface markers, showing positive rates of CD9 (52.78% ± 8.15%), CD63 (95.23% ± 3.02%), and CD81 (91.98% ± 5.50%) (Figure 1D). The overall positivity for both CD63 and CD81 markers was 87.53% ± 7.21%, with 50.95% ± 9.07% of the exosomes also co-positive for CD9 (Figure 1E).

Effects of hypADSC-Exo on the Morphology and Size of UV-Induced Senescent HDFs

HDFs isolated from human abdominal skin samples appeared as elongated spindle-shaped (Figure 2A1). Flow cytometry analysis of cells showed that isolated cells were highly positive for CD90 (94,64%), Vimentin (98,39%), and S100A4 (97,95%), which had characteristics of fibroblast. At the start of the experiment, 50% of normal spindle-shaped HDFs reached 90% confluence after 72 hours (Figure 2A2). In contrast, senescent HDFs, which initially exhibited a flattened

https://doi.org/10.2147/CCID.S523936

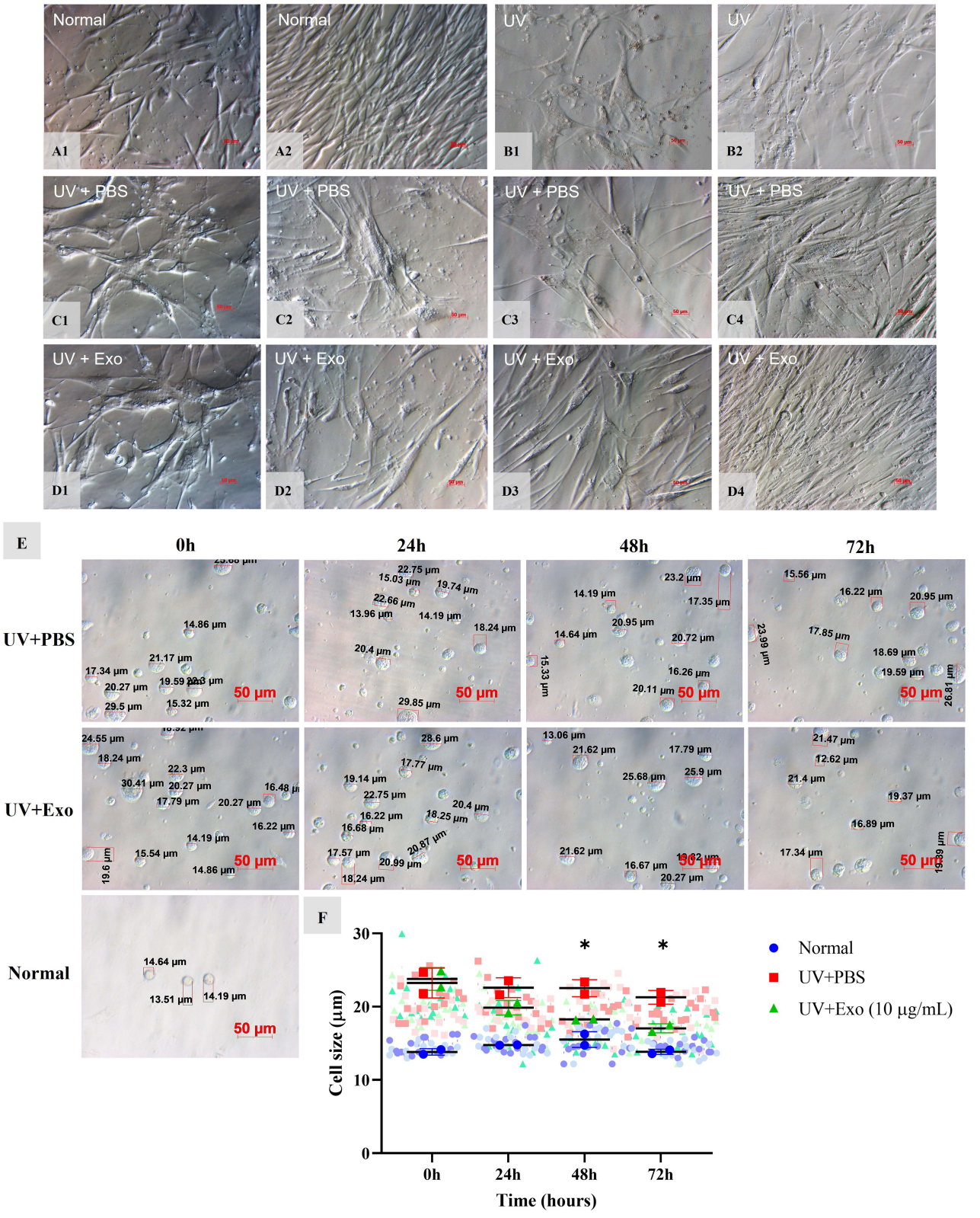

Figure 2 Effects of hypADSC-Exo on HDF morphology and size alteration. Normal 4th passage HDFs at 0 h and 72 h (**A1** and **A2**). UV-induced senescent HDFs at 0 h and 72 h (**B1** and **B2**). Changes of HDF appearance at 0 h, 24 h, 48 h, and 72 h after treatment in the UV+PBS group (**C1–C4**) and UV+Exo group (**D1–D4**). Representative images of two individual experiments. Scale bar = 50 μm. The cell size of the UV+PBS group and UV+Exo group after treatment at 0 h, 24 h, 48 h, and 72 h, compared with normal cells (**E**). Graph of cell size changes between different groups (n=2). Two biological samples, each with sixteen cells, were used. The averages from one experiment of each group are coded in dark blue dots, red squares, and green triangles, whereas individual cell size from a single experimental run is coded in light color in the background. Data are presented as mean (SD); *p<0.05, UV+PBS versus (vs) UV+Exo group, calculated using two-way ANOVA with Turkey's post-test (**F**).

and larger polygonal appearance at 0 hours (Figure 2B1–D1), maintained their distinct morphology and low cell density at 72 hours in the UV (Figure 2B2) and UV+PBS groups (Figure 2C4). After 24 hours of exosome treatment, no significant differences were observed between cells in the UV+PBS group (Figure 2C2) and the UV+Exo group (Figure 2D2). However, by 48 hours, cells in the UV+Exo group displayed improved morphology, with smaller, less polygonal shapes (Figure 2D3), and increased cell proliferation was noted at 72 hours compared to the UV+PBS group (Figure 2C3 and C4).

Regarding cell size, at 0 hours, the average size of cells in the normal group (13.8±0.4 μm) was significantly smaller than those in the UV+PBS (23.2±2 μm) and UV+Exo (23.8±1.5 μm) groups ($p<0.05$) (Figure 2E and F). At 48 hours, cell size in the UV+Exo group (18.2±0.1 μm) was significantly smaller compared to the UV+PBS group (22.5±1.2 μm), with $p<0.05$. This trend persisted at 72 hours, with the UV+Exo group (17±0.6 μm) showing smaller cell sizes than the UV +PBS group (21.3±0.9 μm) ($p<0.05$), approaching those in the normal group (13.8±0.4 μm) (Figure 2E and F).

Overall, these results indicate that young HDFs appeared obviously in the hypADSC-Exo-treated group.

Effects of hypADSC-Exo on the Expression of SA-β-Galactosidase Activity

Before treatment, senescent HDFs displayed strong SA-β-galactosidase activity, indicated by blue staining in the UV +PBS, UV+Exo, and UV groups (Figure 3A1, B1 and B6), compared to the normal group (Figure 3B5). At 24 hours post-treatment, no noticeable differences were observed between the UV+PBS and UV+Exo groups (Figure 3A2 and B2). However, at 48 hours, a reduction in SA-β-galactosidase activity was evident in the UV+Exo group compared to the UV+PBS group (Figure 3B3 and A3), and this decrease persisted at 72 hours (Figure 3B4 and A4). These differences were statistically significant at 72 hours ($p<0.05$), with values of 347.7±21.5 for the UV+PBS group and 50.7±30.8 for the UV+Exo group (Figure 3C).

Alamar blue staining revealed stronger absorbance in the UV+Exo group at 24 and 48 hours compared to the UV +PBS group, suggesting improved HDF proliferation in the UV+Exo group. However, by 72 hours, the difference between the UV+PBS and UV+Exo groups was no longer notable, and the absorbance intensity in both groups was lower than that of the normal group (Figure 3D). Additionally, at 48 hours, further investigation of senescence-associated gene expression showed that the mRNA levels of p16 and p21 were significantly downregulated in the UV+Exo group compared to the UV+PBS group ($p<0.05$) (Figure 3E). These results suggest that hypADSC-Exo could reverse the senescence of HDFs after 48 hours of treatment.

Effects of hypADSC-Exo on Skin Appearance and Barrier Functions of Photoaged Mice

To investigate the effects of hypADSC-Exo on ameliorating photoaging morphology, exosomes were topically applied to the shaved backs of mice twice a week for six consecutive weeks (Figure 4A). Microscopic photos were taken every two weeks to observe skin appearance. At week 0, all UV-induced mice exhibited dry, leathery skin with deep horizontal wrinkles (Figure 4C1–G1), while the normal group displayed smooth skin (Figure 4B1), confirming the successful establishment of the photoaging model.

By week 2, the skin of mice in the tretinoin group showed redness and scaliness, consistent with common side effects of the drug (Figure 4G2). Mice in all other groups, except for the normal group (Figure 4B2), still displayed pronounced aging signs with furrows (Figure 4C2–F2). However, continued administration of hypADSC-Exo resulted in visible skin improvements, particularly in the Exo2 group (hypADSC-Exo 100 μg/mL) by week 4, with fewer wrinkles (Figure 4F3), resembling those in the tretinoin group (Figure 4G3). In contrast, no significant changes were observed in the PBS (Figure 4D3) or Exo1 group (Figure 4E3) compared to the UV group (Figure 4C3).

By week 6, the skin of mice in the Exo2 (Figure 4F4) and tretinoin groups (Figure 4G4) appeared smoother and nearly wrinkle-free, similar to the normal group, although not as pink (Figure 4B4). Deep wrinkles remained evident in the other groups (Figure 4C4–E4).

A line graph of Bissett wrinkle scores showed that at week 0, the normal group had a low score of 0.8±0.4, significantly different from the UV group (2.8±0.4, $p<0.0001$). At week 2, the Exo2 group showed a significant reduction in score (2±0.6) compared to the UV group (3±0, $p<0.05$), but no significant difference compared to the tretinoin group (2.3±0.5). By week 4, the scores in the Exo1, Exo2, and tretinoin groups had dropped to 1.8±0.4, 1.5±0.5, and 1.7±0.5, respectively, all significantly

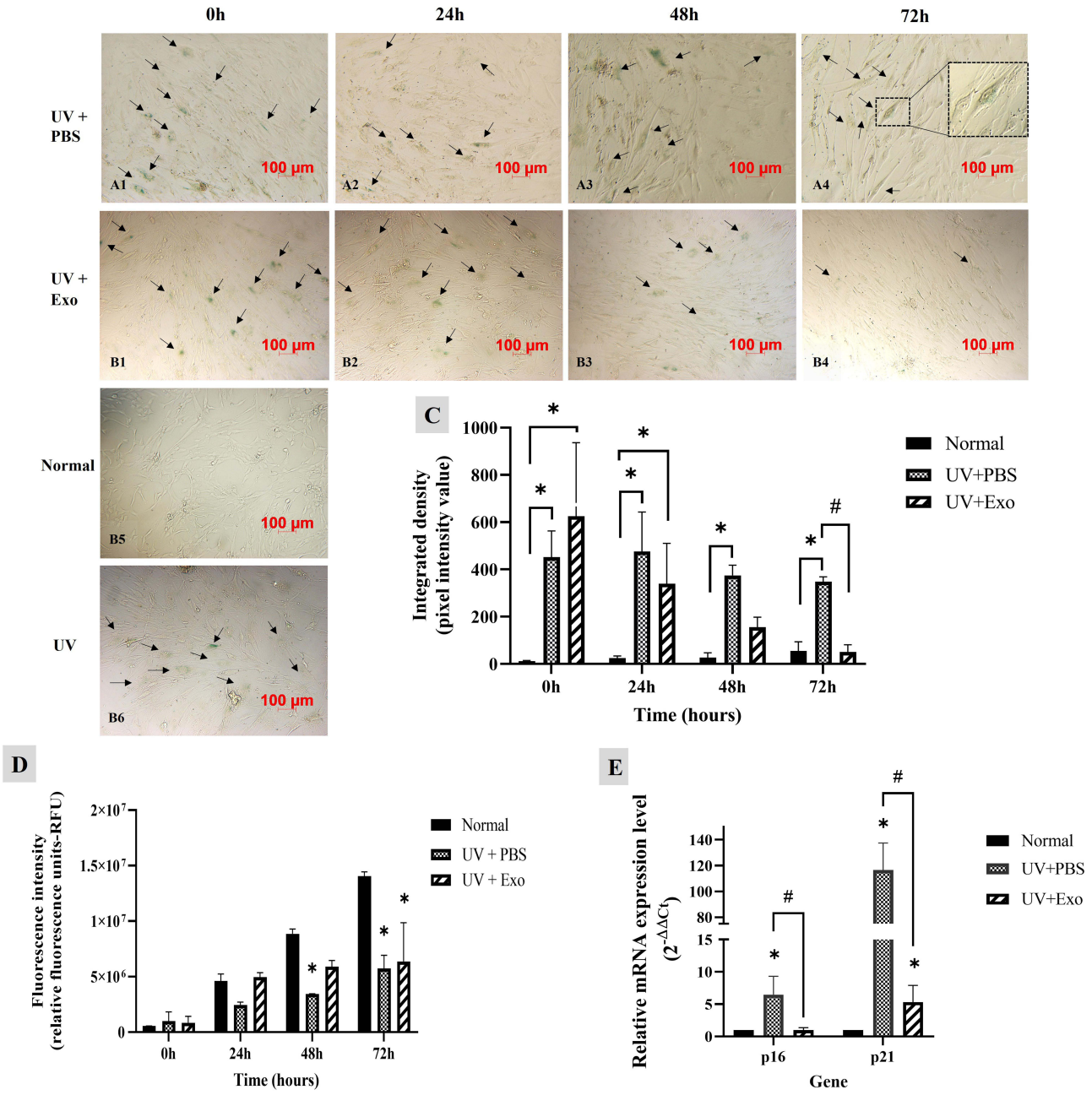

Figure 3 Effects of hypADSC-Exo on HDFs senescent phenotype and function. SA-β-galactosidase activity in senescent HDFs treated with PBS (**A1**–**A4**) and hypADSC-Exo (**B1**–**B4**) at different time points, representative images of three independent experiments, scale bar = 100 μm. Representative images of SA-β-gal staining in HDFs from the normal group (**B5**) and the UV-induced senescence group (**B6**). SA-β-galactosidase signals intensity analyzed by Image J (n=3, *p<0.05, vs normal group; #p<0.05, vs UV+PBS group). Data are presented as mean (SD), calculated using two-way ANOVA with Turkey's post-test. Three biological replicates, each with two technical replicates, were used (**C**). Cell proliferation was assessed at different time points using Alamar blue staining (n=2; *p<0.05, vs normal group). Data are presented as mean (SD), calculated using two-way ANOVA with Turkey's post-test. Two biological replicates, each with three technical replicates, were used (**D**). mRNA expression of p16 and p21 were determined by RT-qPCR at 48 h (n=5; *p<0.05, vs normal group; #p<0.05, UV+PBS vs UV+Exo group). Data are presented as mean (SEM), calculated using the Mann–Whitney test. Five biological replicates, each with a single technical replicate, were used (**E**).

lower than the UV group (p<0.0001). These differences persisted through week 6, with low wrinkle scores in the Exo1 (1.8±0.4), Exo2 (1.3±0.5), and Tretinoin (1.3±0.5) groups compared to the UV group (p<0.0001). However, wrinkle scores in the Exo1, Exo2, and Tretinoin groups remained significantly higher than those in the normal group (p<0.05) (Figure 4H).

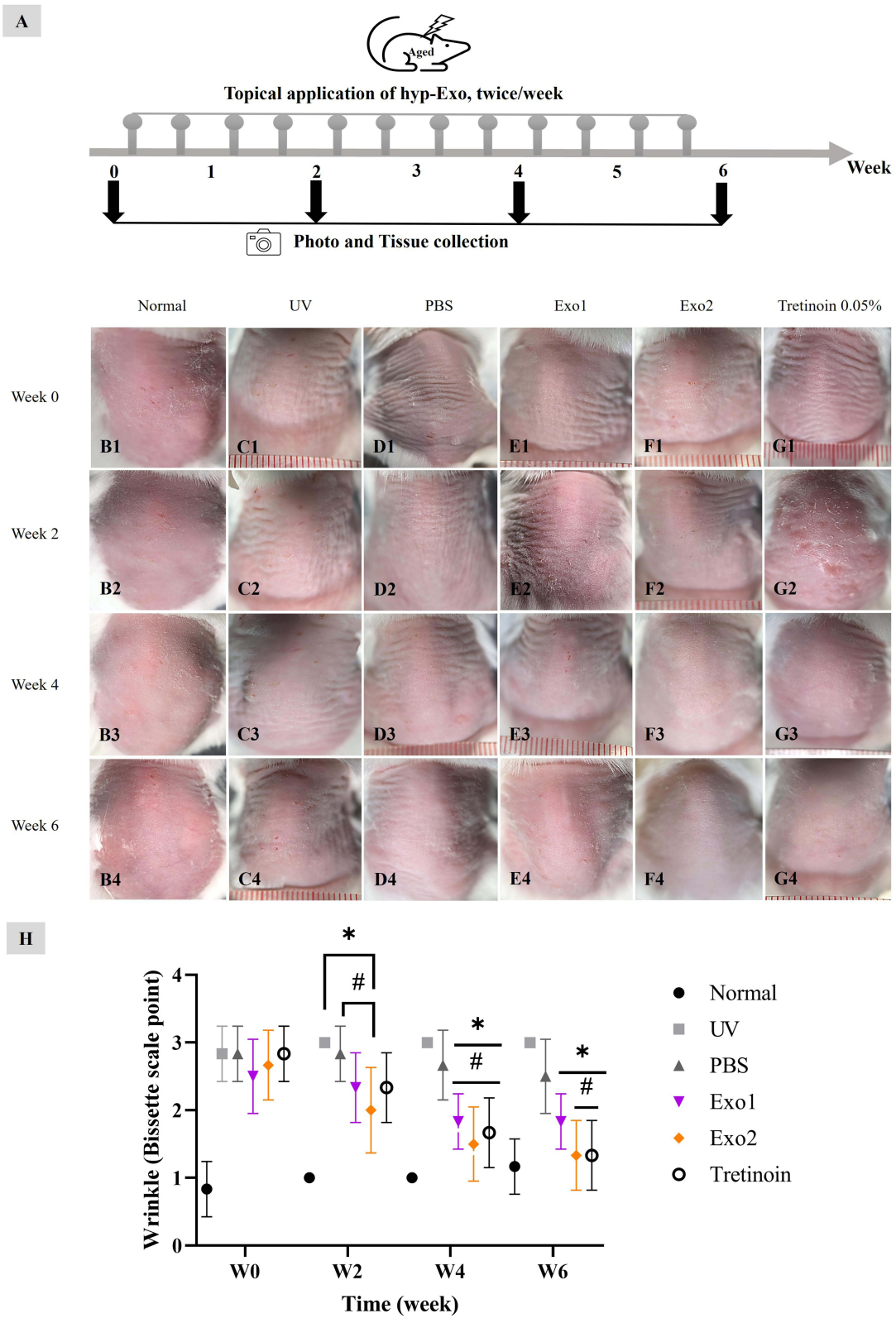

Figure 4 Effects of hypADSC-Exo on the skin appearance of photoaged mice. Schematic representation and timeline of the experiment (**A**); Changes in the skin surface appearance of normal mice at different time points (**B1**–**B4**); UV-induced photoaged mice (**C1**–**C4**); PBS-treated mice (**D1**–**D4**); Exo1-treated group (hypADSC-Exo 50 μg/mL) (**E1**–**E4**); Exo2-treated group (hypADSC-Exo 100 μg/mL) (**F1**–**F4**); Tretinoin 0.05%-treated group (**G1**–**G4**); Wrinkle scores assessed using the Bissett scale across different groups and time points (n=6; *p<0.05, vs UV group; #p<0.05, vs PBS group) (**H**). Data are presented as mean (SD), calculated using repeated two-way ANOVA with Turkey's post test. Six biological replicates, each with three technical replicates, were used. W, week.

https://doi.org/10.2147/CCID.S523936

Overall, these results demonstrate that hypADSC-Exo at a 100 μg/mL dose (Exo2) significantly reduced photoaging signs by week 2, earlier than the effects observed in the tretinoin group, indicating the promising regenerative potential of hypADSC-Exo.

The cutaneous structure and barrier functions are key indicators of photoaged skin status. As shown in Figure 5A, at week 0, skin hydration values in the normal group were 31.2 ± 5.6, while in the UV group, these values significantly decreased to 14.8 ± 2.2. Meanwhile, skin thickness and pinch test values were 0.6 ± 0.1 and 1 ± 0, respectively, in the normal group, but significantly increased to 1 ± 0.1 and 1.7 ± 0.5 in the UV group ($p<0.001$, Figure 5B and C). These data highlight the substantial degradation of barrier function caused by excessive UV irradiation.

After topical treatment with hypADSC-Exo, gradual improvements were observed, with significant enhancements in the Exo2 group. At week 6, HypADSC-Exo increased skin hydration levels to 25 ± 2, while reducing skin thickness and pinch test values to 0.7 ± 0.1 and 1.3 ± 0.3, respectively, compared to the UV group, which showed values of 12.6 ± 4.3, 1 ± 0.08, and 2.9 ± 0.5 ($p<0.05$). These findings indicate that hypADSC-Exo significantly restores the barrier function in photoaged skin.

Effects of hypADSC-Exo on the Pathological Impairments of Photoaged Skin

The administration of hypADSC-Exo significantly alleviated histopathological impairments in photoaged skin. As seen in Figure 6A and B, normal skin displayed a thin epidermis with few keratinocyte layers, orderly arranged fibroblasts, and collagen fibers with a wavy structure.

In contrast, the UV group exhibited marked pathological changes, including epidermal hyperplasia and collagen degradation (Figure 6C1–G1). At week 2, no significant changes were observed in the UV, PBS, Exo1, and Exo2 groups (Figure 6C2–F2), while the tretinoin group showed an increase in epidermal thickness (Figure 6G2). By week 4, thickened epidermis persisted in all groups (Figure 6C3–G3). At week 6, the epidermal thickness in the Exo1, Exo2,

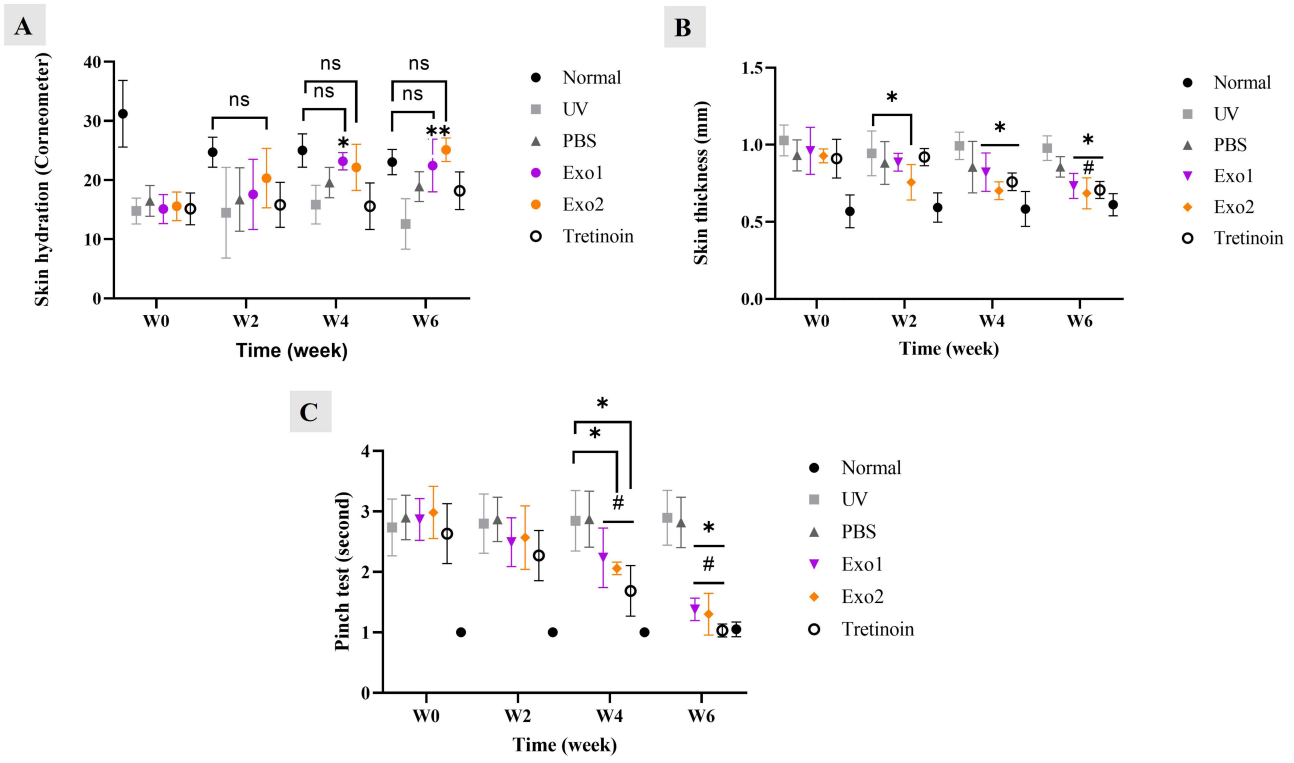

Figure 5 Effects of hypADSC-Exo on skin structure and barrier function of photoaged mice. Skin hydration levels of multiple groups measured by Corneometer device (n=6; *p<0.05, vs UV group, ns: not significant) (**A**). Skinfold thickness changes at different time points (n=6; *p<0.05, vs UV group; #p<0.05, vs PBS group) (**B**). Skin elasticity detected by pinch test of multiple groups (n=6; *p<0.05, vs UV group; #p<0.05, vs PBS group) (**C**). Data are presented as mean (SD), calculated using repeated two-way ANOVA with Turkey's post test. Six biological replicates, each with three technical replicates, were used. W, week.

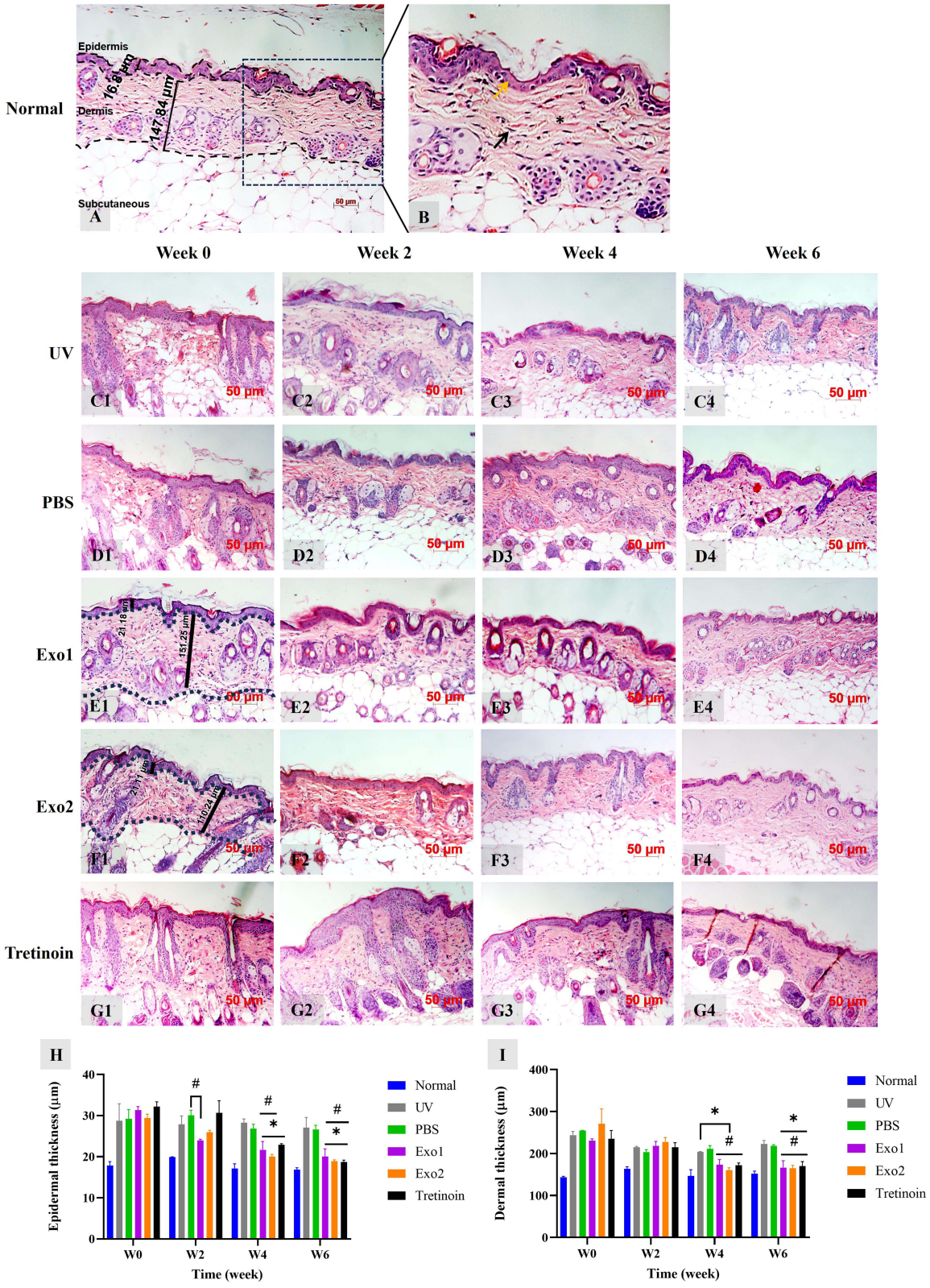

Figure 6 Effects of hypADSC-Exo on the pathological impairments of photoaging skin. Representative photograph of normal group sections stained by hematoxylin and eosin (**A**). Normal skin close-up photograph, yellow arrow: thin epidermis with 1–3 cell layers, black arrow: fibroblast interspersed with collagen fibers, and asterisk: collagen bundles oriented wavy parallel to the skin surface (**B**). Representative histological images of UV (**C1–C4**), PBS (**D1–D4**), Exo1 (**E1–E4**), Exo2 (**F1–F4**), tretinoin (**G1–G4**) group at different time points. W, week. Epidermal (**H**) and dermal thickness (**I**) changes of multiple groups at different time points (n=2; *p<0.05, vs UV group; #p<0.05, vs PBS group). Data are presented as mean (SD), calculated using two-way ANOVA with Turkey's post test. Two biological replicates, each with three technical replicates, were used. W, week.

https://doi.org/10.2147/CCID.S523936

and tretinoin groups had visibly decreased (Figure 6E4–G4), whereas no changes were noted in the UV and PBS groups (Figure 6C4 and D4).

Notably, epidermal thickness increased from 17.7 ± 0.9 μm in the normal group to 28.8 ± 4.1 μm in the UV group ($p < 0.0001$, Figure 6H). After hypADSC-Exo administration, significant reductions in epidermal hyperplasia were observed at weeks 4 and 6, with thickness in the Exo1 and Exo2 groups decreasing to 20 ± 1.9 μm and 18.9 ± 0.3 μm, respectively ($p < 0.05$), nearly aligning with the tretinoin group's thickness of 18.7 ± 0.4 μm (Figure 6H). Furthermore, dermal thickness in the Exo1, Exo2, and tretinoin groups was significantly reduced compared to the UV and PBS groups in weeks 4 and 6 (Figure 6I).

Masson's Trichrome staining revealed densely packed, wavy collagen fibers with a deep blue-green hue in the normal group (Figure 7A). In contrast, the UV group exhibited fragmented, light blue-green collagen fibers, indicative of a significant reduction in collagen density (Figure 7C1–G1). Quantitative analysis showed that at week 0, the collagen intensity in the normal group was 6017.7 ± 557, which significantly decreased to 1850.9 ± 275 in the UV group ($p < 0.0001$, Figure 7B).

At week 2 post-treatment, no noticeable changes in collagen quantity were observed between the UV, PBS, Exo1, Exo2, and tretinoin groups (Figure 7C2–G2). By week 4, however, collagen density improved in the Exo1, Exo2, and tretinoin groups (Figure 7E3–G3), compared to the UV and PBS groups (Figure 7C3 and D3).

By week 6, continued collagen degradation was evident in the UV and PBS groups, with disorganized fibers and blank spaces (Figure 7C4 and D4). In contrast, the Exo2 group showed a significant increase in collagen intensity, reaching 5033.3 ± 1159.9, compared to 1964.7 ± 341.7 in the UV group ($p < 0.001$) and 1699.4 ± 262 in the PBS group ($p < 0.001$, Figure 7B). This demonstrates that the loss of collagen fibrils was notably alleviated, and the damaged dermal structure was visibly repaired in the Exo1 and Exo2 groups (Figure 7E4 and F4), similar to the tretinoin group (Figure 7G4).

These findings underscore the capacity of hypADSC-Exo to modulate and restore the structural integrity of photoaged skin.

Effects of hypADSC-Exo on Gene Expression of Collagen 1, 3, and MMPs

As illustrated in Figure 8A, the mRNA expression levels of collagen types 1 and 3 were significantly reduced in the UV group (0.1 ± 0.07 and 0.2 ± 0.1, respectively) compared to the normal group (1 ± 0, $p < 0.05$). Treatment with hypADSC-Exo at the Exo2 dose led to an increase in collagen 1 and 3 expression levels (0.7 ± 0.6 and 1.3 ± 0.7, respectively), which were higher than those in the Exo1 group (0.006 ± 0.006 and 0.5 ± 0.2) and the UV group, although these differences were not statistically significant. The PBS group (0.2 ± 0.1 and 0.6 ± 0.4) and the tretinoin group (0.7 ± 0.3 and 0.3 ± 0.1) did not exhibit clear trends in collagen expression.

Furthermore, UV irradiation caused a notable increase in the mRNA expression of MMP-1, MMP-2, and MMP-3 in the UV group compared to the normal group (2.2 ± 1.1, 1.8 ± 0.7, and 1.3 ± 1.3, respectively). Following hypADSC-Exo treatment, MMP-1, MMP-2, and MMP-3 expression in the Exo2 group decreased to 0.8 ± 0.4, 0.1 ± 0.06, and 0.6 ± 0.4, respectively. Although these reductions were notable compared to the PBS and tretinoin groups, the differences were not statistically significant ($p > 0.05$, Figure 8B). In summary, these results show that hypADSC-Exo in dose-dependent manner could increase gene expression of collagen type 1 and 3, while reducing the expression of MMP-1, MMP-2 and MMP-3 in photoaged mouse skin.

Discussion

hypADSC-Exo exhibited a cup-shaped morphology, consistent with prior findings on extracellular vesicles, with a mean diameter of 102.3 ± 35.4 nm, classifying them as small extracellular vesicles (under 200 nm). The total exosomal protein yield from 100 mL of ADSC culture media exceeded previous reports.[26] Flow cytometry revealed that EVs expressed key exosomal markers, with positive rates of CD9 (52.78% ± 8.15%), CD63 (95.23% ± 3.02%), and CD81 (91.98% ± 5.50%). A total of 87.53% ± 7.21 of EVs were co-positive for CD63 and CD81, and among these, 50.95% ± 9.07 also expressed CD9. While the positivity rate for CD9 is relatively lower than CD63 and CD81, this phenomenon has also been reported in previous studies. CD9 expression on EVs has been shown to be more variable depending on the cell source, isolation method, and subtypes of EVs.[33] Importantly, according to the MISEV2023 guidelines, exosome

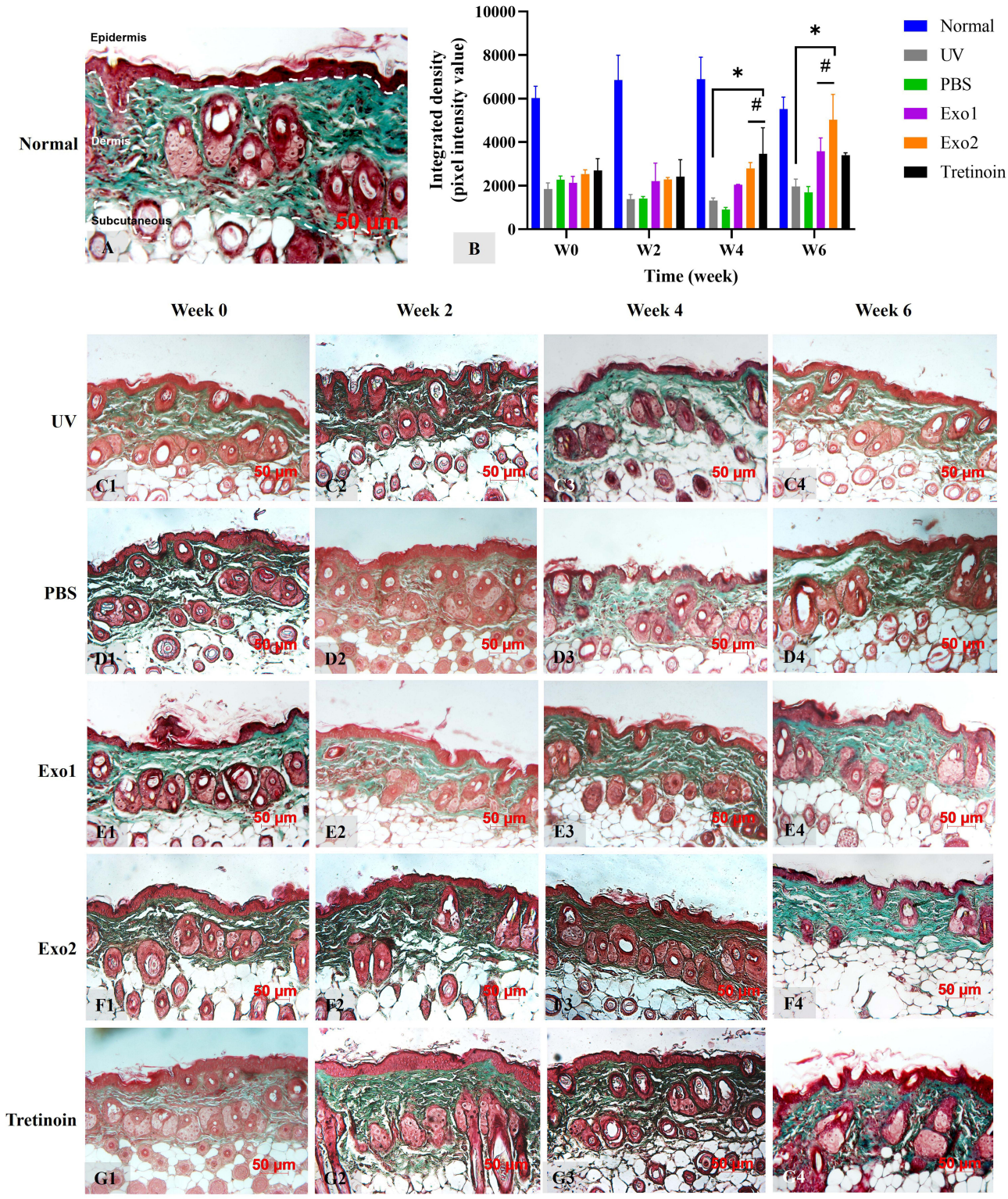

Figure 7 Effects of hypADSC-Exo on the abnormalities of dermis sections in photoaging skin. Representative photographs of normal group sections stained by Masson staining (**A**). Collagen qualification at different time points analyzed by Image J (n=2; *p<0.05, vs UV group; #p<0.05, vs PBS group). Data are presented as mean (SD), calculated using two-way ANOVA with Turkey's post test. Two biological replicates, each with three technical replicates, were used. W, week (**B**). Changes in collagen density of UV (**C1**–**C4**), PBS (**D1**–**D4**), Exo1 (**E1**–**E4**), Exo2 (**F1**–**F4**), and tretinoin group (**G1**–**G4**) over time. Representative images of two independent trials.

https://doi.org/10.2147/CCID.S523936

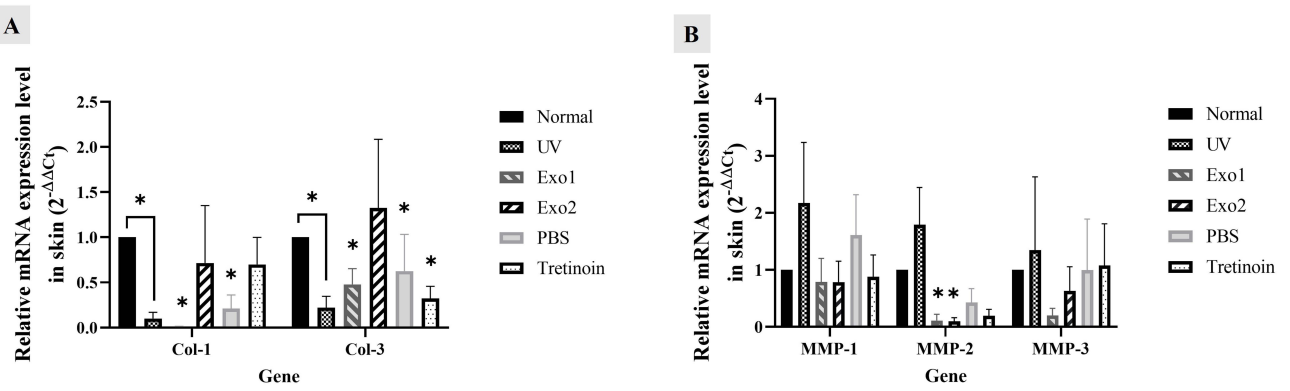

Figure 8 Effects of hypADSC-Exo on gene expression of collagen 1, 3 and MMPs. mRNA expression of collagen 1 and 3 genes of different groups at week 6 (n=5; *p<0.05, vs normal group) (**A**). mRNA expression of MMP-1, MMP-2, and MMP-3 genes among groups at week 6 (n=5; *p<0.05, vs normal group) (**B**). Data are presented as mean (SEM), calculated using Mann–Whitney test. Five biological replicates, each with a single technical replicate, were used.

characterization should involve multiple markers and features. In our study, the co-expression of three canonical tetraspanins, together with consistent size and morphology analysis, supports the identification of the isolated vesicles as exosomes.

The Exo group had more spindle-shaped cells than the UV group and showed significant cell proliferation improvements. The Exo-treated cells were smaller than those in the PBS group. These results likely arise from new cells from non-senescent cells and apoptosis of senescent ones,[34] or reversal of cellular senescence. To better depict the physiological conditions linked with skin aging, we chose not to synchronize the cells before UV exposure. Consequently, UV exposure has minimal impact on cells not in the S phase, creating a mosaic pattern of both senescent and proliferative cells. Over time, the non-senescent cells maintain their ability to proliferate, which explains the presence of dividing cells observed 72 hours after UV treatment. These findings suggest that hypADSC-Exo might enhance HDF proliferation, consistent with prior research,[27] and the effective dose of hypADSC-Exo at 10 μg/mL was similar to the previous study regarding the effect of normoxia-induced ADSC-Exo on promoting skin fibroblast proliferation.[18] However, these results do not support the hypothesis that hypADSC-Exo could reverse cell senescence.

The expression of senescence-associated β-galactosidase (SA-β-gal) was less in the Exo group than in the PBS group, indicating hypADSC-Exo may regenerate senescent cells. Moreover, hypADSC-Exo treatment significantly enhanced cell proliferation. mRNA analysis showed significant downregulation of p16 and p21 in the Exo group. This may be due to hypADSC-Exo reversing senescent HDFs, a phenomenon not previously demonstrated. However, caution is warranted as cell senescence involves complex interactions influenced by various factors.

UV can lead to acute reactions, such as inflammation, sunburn, and tanning, as well as chronic conditions, including photoaging, immunosuppression, and carcinogenesis.[35] In the epidermis, keratinocytes initially respond to UV exposure through the epidermal growth factor receptor, leading to transient epidermal hyperplasia.[36] However, prolonged UV exposure can cause irreversible DNA damage and apoptosis of stem cells in the basal layer and hair bulge, ultimately reducing epidermal thickness.[37] While the dermis thins with intrinsic aging, solar aging causes it to thicken, likely due to the increased volume of dermal cysts (elastosis), fat, glands, and hair follicles, as well as the replacement of collagen fibers with glycosaminoglycans.[38] Consequently, sun-exposed skin tends to be stiffer compared to sun-protected skin of the same age.[39] Acute UV exposure induces angiogenesis in human skin, while chronic UV irradiation diminishes the size and number of cutaneous vessels due to degenerative changes in the upper dermis, affecting vascular structure and function in photoaged skin.[40]

The Exo2 group showed slight improvement in skin wrinkles without side effects, while the tretinoin 0.05% group had severe erythema and scaling. Despite being a standard photoaging treatment, tretinoin often causes skin irritation, leading to poor patient compliance. hypADSC-Exo may enhance skin barrier function and restore elasticity in photo-aged skin dose-dependently. Previous studies were also noted some aspects of aged skin function improvement by using normoxic-induced ADSC-Exo in ameliorating photoaging,[41] however, the data considering hypADSC-Exo role is limited.

The thickened epidermis in photoaged skin decreased in the hypADSC-Exo treatment group. Dermal thickness decreased at weeks 2 and 4 but remained stable from weeks 4 to 6. This trend may be due to reduced large abnormal elastin fibers and glycosaminoglycans, replaced by increased collagen bundles, leading to stable dermal thickness. Collagen density in the Exo2 group was significantly higher than in the UV and PBS groups and superior to the Exo1 group, indicating a more pronounced effect with the Exo2 dose (100 μg/mL). These results agree with Yu-shuai Wang's (2023) findings which showed miR-1246 or LncRNA H19-overexpressing normoxic ADSC-Exo could reduce UVB-induced wrinkle formation and epidermis thickening in Kunming mice.[42,43] Our study applied non-modified hypADSC-Exo topically in different mouse types, unlike previous studies that used modified normoxic ADSC-Exo via tail vein injection. Results indicated an upregulation of collagen 1 and 3 and a downregulation of MMP-1, MMP-2, and MMP-3 in the Exo2 group, though these changes lacked statistical significance. Factors explaining this observation include the ability of hypADSC-Exo to promote fibroblast proliferation and migration by activating the PI3K/AKT pathway.[27] HypADSC-Exo counteracts reactive oxygen species, reduces inflammatory factors, and inhibits collagen degradation via GLRX5 delivery.[28] They also enhance angiogenesis via the VEGF pathway.[26] Given these mechanisms under different conditions, this study further investigates the therapeutic potential of hypADSC-Exo in mitigating photoaging.

The effective dose in our study was lower than in a previous study using hUC-MSC-Exo combined with marine sponge Haliclona sp. spicules (SHSs) as microneedles for treating photoaging. In that study, hUC-MSC-Exo at 100 μg/mL showed mild skin wrinkle improvement compared to the 1 mg/mL group, with treatments every other day for two weeks. Our study, without microneedling, demonstrated that topical hypADSC-Exo at 100 μg/mL (10 μg/8 cm^2) effectively improved skin morphology over six weeks with two treatments per week. These results suggest hypADSC-Exo could be more effective than normoxic UC-MSC-Exo. In contrast, Yu-shuai Wang et al[42,43] demonstrated that normoxic ADSC-Exo at the concentration of 5×10^9 particles/mL/mice, injected three times a week for 4 weeks, proved efficacy in suppressing photoaging. This dose was somewhat lower than that of our study, which administered at dose 8.7×10^9 particles/mice two times a week for six weeks. A possible explanation for this might be due to the difference in administration route, in which the intravenous injection was more beneficial than the topical application in delivering drugs.

Previous studies suggest that exosomes with liposome-like structures penetrate the skin poorly, mostly remaining in the stratum corneum. However, our findings indicate positive effects of topical hypADSC-Exo in treating photoaging.[44] Several factors may explain this: (1) exosomes are absorbed into human skin and could similarly penetrate mouse skin,[45] potentially through follicular absorption, similar to liposomes;[44] (2) the thin stratum corneum of mice (~5 μm[46]), which may be weakened after UV irradiation, reduces skin resistance and increases permeability;[46] (3) the occlusion method used in this study, where the skin was sealed for 30 minutes, along with massage, enhanced skin permeation,[47,48] potentially increasing the penetration depth by a factor of five through the hair follicle infundibula;[44] (4) mechanisms in the stratum corneum, like paracrine signaling between epidermal and dermal cells, may enhance the anti-aging effects of exosomes in superficial layers.[49] Chronic UV irradiation mainly damages fibroblasts in the papillary dermis, with minimal effect on those in the reticular dermis.[50] Thus, exosomes may sufficiently impact cells in the superficial dermis for therapeutic benefits efficacy.

However, our study has certain limitations that warrant further investigation to explore the deeper mechanisms of hypADSC-Exo as a potential therapeutic intervention for photoaging. First, we did not assess the penetration ability of topically applied hypADSC-Exo into the skin, a critical factor for determining the effective absorption of therapeutic substances. Second, the potential impact of specific exosomal cargo, such as miRNAs derived from hypADSC-Exo, and their precise mechanisms of action on HDFs require further examination. Additionally, for clinical application, it is essential to investigate potential side effects and determine the optimal dosage and timing to achieve maximal therapeutic efficacy. These aspects are critical in advancing hypADSC-Exo as a viable treatment option. In conclusion, this might be the first study to evaluate the effects of topical hypADSC-Exo on photoaging. We hope this study lays the groundwork for further research into hypADSC-Exo penetration and mechanisms of action in ameliorating photoaging from the superficial skin layers.

Conclusion

Exosomes derived from hypoxia-induced adipose-derived stem cells (hypADSC-Exo) have demonstrated potential in ameliorating photoaging through topical application. The underlying mechanism by which hypADSC-Exo exerts its effects appears to involve synergistic modulation that reverses the senescence of dermal fibroblasts, leading to the restoration of pathological impairments and enhanced collagen deposition. These properties highlight hypADSC-Exo as a promising therapeutic candidate for the treatment of photoaging, offering potential benefits in restoring skin integrity and reducing signs of aging.

Data Sharing Statement

Processed data and materials used and/or analyzed during the current study are available from the corresponding author on reasonable request.

Ethics Approval and Consent to Participate

The human subjects involved in this research received informed consent. All procedures on human were approved by the Ethics Committee at the University of Medicine and Pharmacy at Ho Chi Minh City (approval no. 56/HĐĐĐ-ĐHYD, date 28/01/2021). The use of animals in the current study was approved by the Institutional Animal Care and Use Committee of Ho Chi Minh National University (approval no. 210103/SCI-AEC, date 20/01/2021).

Acknowledgments

The authors express their gratitude to the Director of VNUHCM-US Stem Cell Institute, University of Science, Vietnam National University Ho Chi Minh City, Vietnam for your support. The authors also thank Dr. Liem Hieu Pham for assistance with skin sample harvesting for fibroblast isolation.

Author Contributions

All authors made a significant contribution to the work reported, whether that is in the conception, study design, execution, acquisition of data, analysis and interpretation, or in all these areas; took part in drafting, revising or critically reviewing the article; gave final approval of the version to be published; have agreed on the journal to which the article has been submitted; and agree to be accountable for all aspects of the work.

Funding

This research is funded by Stem Cell Institute, University of Science, Vietnam National University Ho Chi Minh City (VNU-HCM), Vietnam.

Disclosure

The authors declare no competing interests, financial or otherwise, associated with this publication.

References

1. Farage MA, Miller KW, Berardesca E, Maibach HI. Clinical implications of aging skin: cutaneous disorders in the elderly. *Am J Clin Dermatol*. 2009;10(2):73–86. doi:10.2165/00128071-200910020-00001
2. Addor FAS. Beyond photoaging: additional factors involved in the process of skin aging. *Clin Cosmet Invest Dermatol*. 2018;11:437–443. doi:10.2147/CCID.S177448
3. Knuutinen A, Kokkonen N, Risteli J, et al. Smoking affects collagen synthesis and extracellular matrix turnover in human skin. *Br J Dermatol*. 2002;146(4):588–594. doi:10.1046/j.1365-2133.2002.04694.x
4. Vierkötter A, Schikowski T, Ranft U, et al. Airborne particle exposure and extrinsic skin aging. *J Invest Dermatol*. 2010;130(12):2719–2726. doi:10.1038/jid.2010.204
5. Katta R, Kramer MJ. Skin and Diet: an Update on the Role of Dietary Change as a Treatment Strategy for Skin Disease. *Skin Therapy Lett*. 2018;23(1):1–5.
6. Mekić S, Jacobs LC, Hamer MA, et al. A healthy diet in women is associated with less facial wrinkles in a large Dutch population-based cohort. *J Am Acad Dermatol*. 2019;80(5):1358–1363.e2. doi:10.1016/j.jaad.2018.03.033
7. Farage MA, Miller KW, Elsner P, Maibach HI. Characteristics of the Aging Skin. *Adv Wound Care*. 2013;2(1):5–10. doi:10.1089/wound.2011.0356
8. Kang S, Amagai M, Bruckner AL. *Fitzpatrick's Dermatology*. 9th ed ed. McGrawHill Education; 2019.

9. Yao X, Li H, Chen L, Tan LP. UV-induced senescence of human dermal fibroblasts restrained by low-stiffness matrix by inhibiting NF-κB activation. *Eng Regen*. 2022;3(4):365–373. doi:10.1016/j.engreg.2022.08.002
10. Codriansky KA, Quintanilla-Dieck MJ, Gan S, Keady M, Bhawan J, Rünger TM. Intracellular degradation of elastin by cathepsin K in skin fibroblasts--a possible role in photoaging. *Photochem Photobiol*. 2009;85(6):1356–1363. doi:10.1111/j.1751-1097.2009.00592.x
11. Kapoor KS, Kong S, Sugimoto H, et al. Single extracellular vesicle imaging and computational analysis identifies inherent architectural heterogeneity. *bioRxiv*. 2023:2023.12.11.571132. doi:10.1101/2023.12.11.571132.
12. Cai Y, Li J, Jia C, He Y, Deng C. Therapeutic applications of adipose cell-free derivatives: a review. *Stem Cell Res Ther*. 2020;11(1):312. doi:10.1186/s13287-020-01831-3
13. Fang S, Xu C, Zhang Y, et al. Umbilical Cord-Derived Mesenchymal Stem Cell-Derived Exosomal MicroRNAs Suppress Myofibroblast Differentiation by Inhibiting the Transforming Growth Factor-β/SMAD2 Pathway During Wound Healing. *Stem Cells Transl Med*. 2016;5 (10):1425–1439. doi:10.5966/sctm.2015-0367
14. Wu P, Zhang B, Shi H, Qian H, Xu W. MSC-exosome: a novel cell-free therapy for cutaneous regeneration. *Cytotherapy*. 2018;20(3):291–301. doi:10.1016/j.jcyt.2017.11.002
15. Hu L, Wang J, Zhou X, et al. Exosomes derived from human adipose mensenchymal stem cells accelerates cutaneous wound healing via optimizing the characteristics of fibroblasts. *Sci Rep*. 2016;6(1):32993. doi:10.1038/srep32993
16. Hajialiasgary Najafabadi A, Soheilifar MH, Masoudi-Khoram N. Exosomes in skin photoaging: biological functions and therapeutic opportunity. *Cell Commun Signal*. 2024;22(1):32. doi:10.1186/s12964-023-01451-3
17. Guo JA, Yu PJ, Yang DQ, Chen W. The Antisenescence Effect of Exosomes from Human Adipose-Derived Stem Cells on Skin Fibroblasts. *Biomed Res Int*. 2022;2022:1034316. doi:10.1155/2022/1034316
18. Choi EW, Seo MK, Woo EY, Kim SH, Park EJ, Kim S. Exosomes from human adipose-derived stem cells promote proliferation and migration of skin fibroblasts. *Exp Dermatol*. 2018;27(10):1170–1172. doi:10.1111/exd.13451
19. Gao W, Wang X, Si Y, et al. Exosome Derived from ADSCs Attenuates Ultraviolet B-mediated Photoaging in Human Dermal Fibroblasts. *Photochem Photobiol*. 2021;97(4):795–804. doi:10.1111/php.13370
20. Gao W, Yuan LM, Zhang Y, et al. miR-1246-overexpressing exosomes suppress UVB-induced photoaging via regulation of TGF-β/Smad and attenuation of MAPK/AP-1 pathway. *Photochem Photobiol Sci*. 2023;22(1):135–146. doi:10.1007/s43630-022-00304-1
21. Pulido-Escribano V, Torrecillas-Baena B, Camacho-Cardenosa M, Dorado G, Gálvez-Moreno MÁ, Casado-Díaz A. Role of hypoxia preconditioning in therapeutic potential of mesenchymal stem-cell-derived extracellular vesicles. *World J Stem Cells*. 2022;14(7):453–472. doi:10.4252/wjsc.v14.i7.453
22. Xue C, Shen Y, Li X, et al. Exosomes Derived from Hypoxia-Treated Human Adipose Mesenchymal Stem Cells Enhance Angiogenesis Through the PKA Signaling Pathway. *Stem Cells Dev*. 2018;27(7):456–465. doi:10.1089/scd.2017.0296
23. Shao C, Yang F, Miao S, et al. Role of hypoxia-induced exosomes in tumor biology. *Mol Cancer*. 2018;17(1):120. doi:10.1186/s12943-018-0869-y
24. Shi R, Jin Y, Zhao S, Yuan H, Shi J, Zhao H. Hypoxic ADSC-derived exosomes enhance wound healing in diabetic mice via delivery of circ-Snhg11 and induction of M2-like macrophage polarization. *Biomed Pharmacother*. 2022;153:113463. doi:10.1016/j.biopha.2022.113463
25. He G, Peng X, Wei S, et al. Exosomes in the hypoxic TME: from release, uptake and biofunctions to clinical applications. *Mol Cancer*. 2022;21 (1):19. doi:10.1186/s12943-021-01440-5
26. Han Y, Ren J, Bai Y, Pei X, Han Y. Exosomes from hypoxia-treated human adipose-derived mesenchymal stem cells enhance angiogenesis through VEGF/VEGF-R. *Int J Biochem Cell Biol*. 2019;109:59–68. doi:10.1016/j.biocel.2019.01.017
27. Wang J, Wu H, Peng Y, et al. Hypoxia adipose stem cell-derived exosomes promote high-quality healing of diabetic wound involves activation of PI3K/Akt pathways. *J Nanobiotechnology*. 2021;19(1):202. doi:10.1186/s12951-021-00942-0
28. Liu Y, Wang Y, Yang M, et al. Exosomes from hypoxic pretreated ADSCs attenuate ultraviolet light-induced skin injury via GLRX5 delivery and ferroptosis inhibition. *Photochem Photobiol Sci*. 2024;23(1):55–63. doi:10.1007/s43630-023-00498-y
29. Cuc HB, Vu BN, Van PP, Trung VT. Establishment of aged human dermal fibroblasts by ultraviolet irradiation. *T?p Chí Y H?c Vi?t Nam*. 2024;544 (2). doi:10.51298/vmj.v544i2.11937
30. Bissett DL, Hannon DP, Orr TV. An animal model of solar-aged skin: histological, physical, and visible changes in UV-irradiated hairless mouse skin. *Photochem Photobiol*. 1987;46(3):367–378. doi:10.1111/j.1751-1097.1987.tb04783.x
31. Chen Y, Yu Q, Xu CB. A convenient method for quantifying collagen fibers in atherosclerotic lesions by ImageJ software. *Int J Clin Exp Med*. 2017;10:14927–14935.
32. Livak KJ, Schmittgen TD. Analysis of relative gene expression data using real-time quantitative PCR and the 2(-Delta Delta C(T)) Method. *Methods*. 2001;25(4):402–408. doi:10.1006/meth.2001.1262
33. Andreu Z, Yáñez-Mó M. Tetraspanins in extracellular vesicle formation and function. *Front Immunol*. 2014;5:442. doi:10.3389/fimmu.2014.00442
34. Zhao H, Traganos F, Darzynkiewicz Z. Kinetics of the UV-induced DNA damage response in relation to cell cycle phase. Correlation with DNA replication. *Cytom Part a J Int Soc Anal Cytol*. 2010;77(3):285–293. doi:10.1002/cyto.a.20839
35. Brenner M, Hearing VJ. The protective role of melanin against UV damage in human skin. *Photochem Photobiol*. 2008;84(3):539–549. doi:10.1111/j.1751-1097.2007.00226.x
36. El-Abaseri TB, Putta S, Hansen LA. Ultraviolet irradiation induces keratinocyte proliferation and epidermal hyperplasia through the activation of the epidermal growth factor receptor. *Carcinogenesis*. 2006;27(2):225–231. doi:10.1093/carcin/bgi220
37. Tang Z, Tong X, Huang J, Liu L, Wang D, Yang S. Research progress of keratinocyte-programmed cell death in UV-induced Skin photodamage. *Photodermatol Photoimmunol Photomed*. 2021;37(5):442–448. doi:10.1111/phpp.12679
38. Kligman LH. The hairless mouse model for photoaging. *Clin Dermatol*. 1996;14(2):183–195. doi:10.1016/0738-081x(95)00154-8
39. Lynch B, Pageon H, Le Blay H, et al. A mechanistic view on the aging human skin through ex vivo layer-by-layer analysis of mechanics and microstructure of facial and mammary dermis. *Sci Rep*. 2022;12(1):849. doi:10.1038/s41598-022-04767-1
40. Chung JH, Eun HC. Angiogenesis in skin aging and photoaging. *J Dermatol*. 2007;34(9):593–600. doi:10.1111/j.1346-8138.2007.00341.x
41. Liang JX, Liao X, Li SH, et al. Antiaging Properties of Exosomes from Adipose-Derived Mesenchymal Stem Cells in Photoaged Rat Skin. *Biomed Res Int*. 2020;2020(1):6406395. doi:10.1155/2020/6406395
42. Gao W, Yuan L, Zhang Y, et al. miR-1246-overexpressing exosomes improve UVB-induced photoaging by activating autophagy via suppressing GSK3β. *Photochem Photobiol Sci*. 2024;23(5):957–972. doi:10.1007/s43630-024-00567-w

43. Gao W, Zhang Y, Yuan L, Huang F, Wang YS. Long Non-coding RNA H19-Overexpressing Exosomes Ameliorate UVB-Induced Photoaging by Upregulating SIRT1 Via Sponging miR-138. *Photochem Photobiol*. 2023;99(6):1456–1467. doi:10.1111/php.13801
44. Trauer S, Richter H, Kuntsche J, et al. Influence of massage and occlusion on the ex vivo skin penetration of rigid liposomes and invasomes. *Eur J Pharm Biopharm*. 2014;86(2):301–306. doi:10.1016/j.ejpb.2013.11.004
45. Kim YJ, Yoo SM, Park HH, et al. Exosomes derived from human umbilical cord blood mesenchymal stem cells stimulates rejuvenation of human skin. *Biochem Biophys Res Commun*. 2017;493(2):1102–1108. doi:10.1016/j.bbrc.2017.09.056
46. Milosheska D, Roškar R. Use of Retinoids in Topical Antiaging Treatments: a Focused Review of Clinical Evidence for Conventional and Nanoformulations. *Adv Ther*. 2022;39(12):5351–5375. doi:10.1007/s12325-022-02319-7
47. Zhai H, Maibach H. Occlusion vs. Skin barrier function. *Skin Res Technol*. 2002;8(1):1–6. doi:10.1046/j.0909-752x.2001.10311.x
48. Zhai H, Maibach H. Effects of Skin Occlusion on Percutaneous Absorption: an Overview. *Skin Pharmacol Appl Skin Physiol*. 2001;14(1):1–10. doi:10.1159/000056328
49. Wang Y, Pching T, Xu X, Zhou S. Protective function of adipocyte-derived extracellular vesicles and adipose stem cells in damage repair and regeneration. *Chinese J Plast Reconstr Surg*. 2025;7(1):35–44. doi:10.1016/j.cjprs.2024.11.007
50. Rognoni E, Goss G, Hiratsuka T, et al. Role of distinct fibroblast lineages and immune cells in dermal repair following UV radiation-induced tissue damage. *Elife*. 2021;10:e71052. doi:10.7554/eLife.71052